

NEW ADVANCES FOR THE ${}^3\text{He}({}^4\text{He},\gamma){}^7\text{Be}$ SOLAR FUSION REACTION*

B.S. NARA SINGH

Department of Physics, University of York, Heslington, York, YO10 5DD, UK
and
Manipal Center for Natural Sciences, Manipal University
Manipal, 576104, Karnataka, India

(Received January 9, 2013)

We present the current status of the available data and the calculations for the cross section of the ${}^3\text{He}(\alpha, \gamma){}^7\text{Be}$ reaction — accurate knowledge of which is required for the solar neutrino flux and the primordial ${}^7\text{Li}$ abundance calculations. Precision measurements are being carried out by us in the range of $E_{\text{cm}} = 1$ to 3 MeV using two types of experimental methods. A brief account of this work is given together with some of the recent theoretical calculations.

DOI:10.5506/APhysPolB.44.511

PACS numbers: 25.40.Lw, 26.20.Fj, 26.35.+c, 26.65.+t

1. Introduction

The ${}^3\text{He}(\alpha, \gamma){}^7\text{Be}$ reaction rate has a significant influence on different fields of physics [1–3]. Consequently, it has been a subject of interest for more than five decades. Studies have been driven both on the experimental and the theoretical fronts, primarily, due to the role of the reaction rate as an essential input to the solar neutrino flux and ${}^7\text{Li}$ abundance calculations [4–20]. A summary of the experimental data and the calculations of $S_{34}(E)$ adopted from some of the representative works is shown in Fig. 1, which highlights the present situation. Here, the S_{34} -factor (in keV b) at a center of mass energy, E (in keV), is related to the cross section, $\sigma_{34}(E)$ (in barns), by $S_{34}(E) = E\sigma_{34}(E)\exp(164.12/E^{1/2})$. In general, the existing results suffer from inconsistencies that yield large uncertainties in the S_{34} -factor extrapolated to zero energy ($S_{34}(0)$) [6, 21]. The Weizmann group attempted to settle down the discrepancies seen in the data, for example, shown in

* Presented at the Zakopane Conference on Nuclear Physics “Extremes of the Nuclear Landscape”, Zakopane, Poland, August 27–September 2, 2012.

Fig. 1(b) [7] and improve the situation by accurately fixing the absolute values of S_{34} around 1 MeV. In this work, it is also stressed that the major observed disagreements between the individual data sets could be attributed to the systematic uncertainties arising from various components of the setups used for the measurements. Since then, a large volume of data have been obtained using three different methods, namely, the detection of the prompt γ rays resulting from the reaction, the offline measurement of the γ activity following the decay of the ${}^7\text{Be}$ nuclei and the direct counting of the ${}^7\text{Be}$ nuclei. Most of the measurements were carried out in the energy range

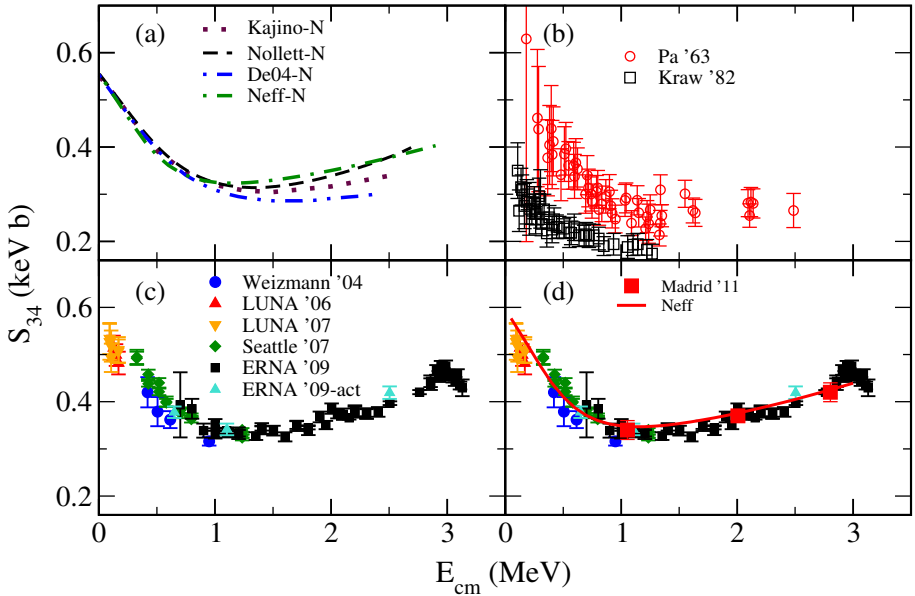


Fig. 1. Representative data and calculations of S_{34} . (a) The theoretical calculations based on the works from Refs. [15] (Kajino-N), [16] (Nolllett-N), [17] (De04-N) and [19] (Neff-N). The $S_{34}(E)$ curves, which have been normalized so as to give $S_{34}(0) = 0.553 \text{ keV b}$, show significant differences in their shapes. (b) Data from Refs. [4] (Pa'63) and [5] (Kraw'82). A large discrepancy between the two sets is evident. Such results yield up to 17% uncertainty in the value of $S_{34}(0)$. (c) Data from Refs. [7] (Weizmann'04), [8] (LUNA'06), [9] (LUNA'07), [10] (Seattle'07) and [12] (ERNA'09, ERNA'09-act). Clearly, the energy dependence observed in the ERNA work above 1 MeV is different from that seen in (b) and in (a) for the curve De04-N. (d) The same as (c) except that the calculations from Ref. [19] (Neff) without any normalization and the new data obtained from our γ activity work [22] (Madrid'11) are also included. A good agreement can be seen between our work and the data from the ERNA Collaboration [12].

of 0.1 to 1.5 MeV and data with much improved accuracies became available (*cf.* Fig. 1). Some inconsistencies can still be seen in the data, in particular in the results above 1 MeV from Refs. [4, 12], that could lead to uncertainties in the value of $S_{34}(0)$ larger than the 5% level recommended in Ref. [2]. See Fig. 1 for details.

To provide independent data and fix the energy dependence of the S_{34} -factor above 1 MeV, where only two conflicting sets of data from Refs. [4] and [12] exist, we initiated two measurements by employing two different techniques, namely, the activity and the recoil detection methods. Here, we present a summary of our activity work [22] (Fig. 1 (d), Madrid'11) and our progress towards measuring the cross sections using the Detector of Recoils And Gammas Of Nuclear reactions (DRAGON) recoil mass separator at TRIUMF [23–25].

2. Experiments and results

2.1. Activity method

A detailed discussion of the setup and the results is presented in Ref. [22]. Here, we give only a few relevant details. An accurate control over the experimental parameters was possible and the systematic errors could be minimized due to the simplicity of our setup. The ${}^3\text{He}$ beam, from the accelerator at Centro de MicroAnálisis de Materiales (CMAM) in Madrid, impinged on a ${}^4\text{He}$ gas target that was isolated from the beam line vacuum and was confined to be inside a chamber by using an Ni foil. Following the capture reaction, the ${}^7\text{Be}$ nuclei traveled along the beam direction and got implanted in a Cu catcher that had been placed after the ${}^4\text{He}$ gas target. Typically, each of our measurements could be completed in less than one day using a 100 to 150 pA beam current due to the μb -level cross sections at medium energies. The Cu catchers were transported, usually within a few days after such ${}^7\text{Be}$ production and implantation runs, to a well calibrated and controlled γ counting setup placed in a low background environment for the activity measurement. The cross section can be deduced accurately from the observed γ activity because it arises from the well studied deexcitation of the 477.6 keV level in ${}^7\text{Li}$ populated by the electron capture of ${}^7\text{Be}$ with a half life of 53.35 (50) days [26] and a branching ratio of 10.44 (4)% [26, 27]. Results from this experiment at three different energies in the range of 1 to 3 MeV are shown in Fig. 1 (d) (Madrid'11). It is evident that, while in agreement with the ERNA work (ERNA'09, ERNA'09-act) [12], our data do not agree with those from Ref. [4]. In order to confirm our results, further measurements covering $E_{\text{cm}} = 0.4$ to 3 MeV are planned in the future.

2.2. Recoil detection method

Our recoil detection measurements were carried out at the TRIUMF laboratory in Vancouver using 3.5, 5.2 and 6.7 MeV ^4He beams. The experimental setup was fairly complex in contrast to that used for our activity work. Some details can be found in Refs. [23, 24]. A windowless differentially pumped ^3He gas target was used in conjunction with the two stage DRAGON recoil mass separator [25]. A silicon (Si) detector, at an angle of 30° with respect to the beam direction, detected the elastically scattered particles from an Au foil placed upstream from our target chamber. Typically, these Si spectra were dominated by the scattered beam particles and a value of $\sim 99\%$ for the beam purity was deduced. Two precisely collimated Si detectors ('monitor detectors') were also placed within the target chamber at angles of 30° and 57° with respect to the beam direction for a continuous measurement of the elastically scattered particles. The separator was optimally tuned so as to effectively suppress the beam and efficiently transfer the ^7Be (3^+) recoils from the target chamber to the focal plane, where a Double Sided Si Strip Detector (DSSSD) had been placed for the particle detection. All of the data was collected using an acquisition system with live time, t_l , between 80 to 99%. The capture cross section, σ_{34} , can be deduced from the number of ^7Be recoils detected by the DSSSD, $N_{7\text{Be}}^f$, via the relation $\frac{N_{7\text{Be}}^f}{t_l \epsilon_s q_f} = \sigma_{34} N_p N_t$. Here, N_p , N_t , ϵ_s and q_f are the number of beam particles, the areal number density of the target, the detection efficiency (the product of the separator transmission efficiency and the quantum efficiency of the DSSSD) and the fraction of the recoils in the charge state selected by the separator, respectively. In this paper, we summarize some of our recent results corresponding to these quantities as well as the background contributions to $N_{7\text{Be}}^f$, which must be known with good accuracies in order to minimize the uncertainties in the values of σ_{34} . Some of the details regarding the cross section measurement and the beam suppression of DRAGON for the present reaction can also be found in Refs. [23] and [24], respectively.

The beam intensity, I_p , was measured every one hour by using a Faraday cup placed slightly upstream from the target chamber. N_p could be reliably estimated by normalizing the total number of the scattered particles detected by the 'monitor detectors' (see above) with the rate of the beam particles obtained using I_p [25]. Our initial analysis yields an uncertainty of $\sim 8\%$ in N_p , which would be one of the dominant sources of error.

A measured density profile of our differentially pumped ^3He target using a 3.5% enriched gas was discussed in Ref. [23]. The detected γ -ray yield from a small volume of the target gas, arising from a resonance in the $^3\text{He}(^{12}\text{C}, p\gamma)^{14}\text{N}$ reaction at $E_{\text{cm}} = 2.389, \text{MeV}$, was used to monitor the target den-

sity profile. In the present work, we repeated these measurements using a 12.1 MeV ${}^{12}\text{C}$ beam and a target gas with pressures in the range of 3 to 6 Torr and an isotopic purity better than 99%. The γ rays from the reaction were detected using a collimated BGO detector. As indicated in Fig. 2, all of the events in the spectrum correspond to the 3.38, 3.89, 5.11 and 6.44 MeV prompt γ rays from the reaction. The 511 keV escape peaks can also be seen. In the inset of Fig. 2, the total normalized γ -ray yield of all of the peaks in the spectrum is shown as a function of the detector position relative to the center of the target. In contrast to the expectations, the γ -ray yield (representing the target density) does not go to zero around the positions ± 120 mm. Currently, we do not have an explanation for this result. The theoretical fits ((inset) black/blue and light gray/red curves) give a target length of ~ 125 mm with a 4% uncertainty. This preliminary value together with the continuously monitored pressure of the ${}^3\text{He}$ target gives a $\sim 5\%$ error in N_t .

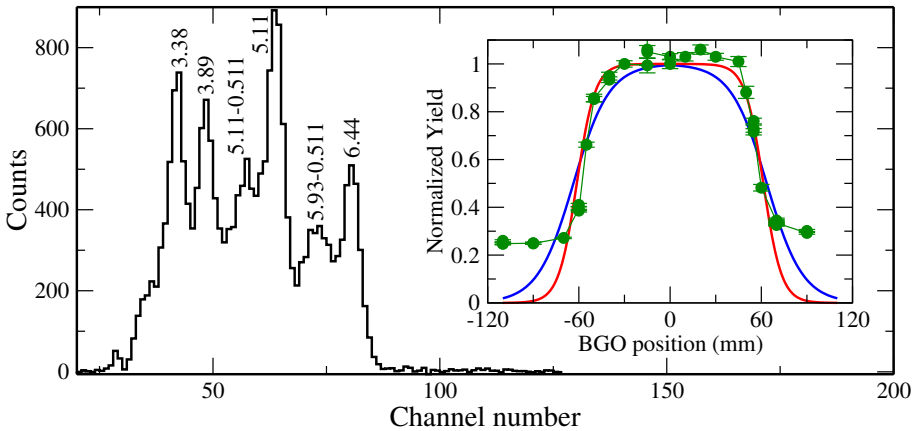


Fig. 2. A typical spectrum of the γ rays, from the ${}^3\text{He}({}^{12}\text{C}, p\gamma){}^{14}\text{N}$ reaction, detected by the BGO detector. (Inset) The normalized total γ -ray yield (green filled circles) as a function of the detector position relative to the center of the target. The light gray/red and black/blue fits give two somewhat different values of 123 and 127 mm, respectively for the length of the gas target. See the text for details.

The acceptance cone angle of the separator was determined by carrying out measurements with an α source placed along the beam axis inside the target chamber. The α particles passed through one of the collimators (having 17, 19 and 21 mrad geometric cone half-angles and a good alignment with the gas target) and the separator before getting detected by the DSSSD. An analysis of the variation of the DSSSD event rate as a function of the collimator solid angle resulted in an acceptance cone half-angle

of 21.0(6) mrad for the separator [23]. This result was also confirmed in a separate experiment via the detection of the ^{17}F recoils in the DSSSD from the $d(^{16}\text{O}, n)$ reaction at beam energies of 922, 952 and 971 A keV. In this case, the DSSSD event rates were analyzed using the well understood inverse kinematics of this reaction, namely, the maximum cone angle of the recoils is 0° at the threshold beam energy of 908.06 A keV and increases gradually with the energy. Two-dimensional histograms, which we refer to as ‘pixel maps’, are shown in Fig. 3. They give the number of implanted ^7Be (3^+) recoils as a function of the DSSSD pixel, *i.e.*, the implantation profile over the area of the DSSSD. Here, a pixel can be identified with the corresponding numbers of x - (on x -axis) and y - (y -axis) strips of the detector. Clearly, the profiles show that the number of implantations are not symmetric with respect to the center of the DSSSD. Such a situation can arise, for example, from the non-optimal settings of the separator and from any misalignments of the centers of the target chamber and the DSSSD relative to the beam axis. Since the cone half-angles of the reaction and the separator acceptance are similar, some of the ^7Be recoils may not be reaching the active area of the DSSSD. This results in an under-counting of the recoils. We are currently performing detailed simulations, in line with those presented in Ref. [28], to reproduce the ‘pixel maps’ (*cf.* Fig. 3) and estimate the loss of the recoils.

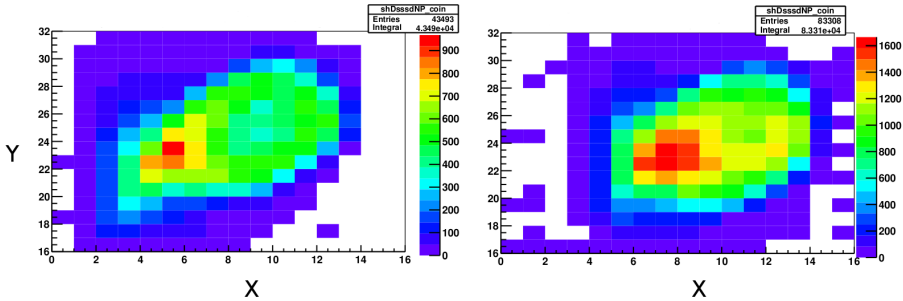


Fig. 3. The ‘pixel maps’ correspond to the measurements carried out at beam energies of 6.7 (left) and 3.5 MeV (right). See the text for details.

The charge state distribution (CSD) studies were carried out by sending ^9Be (2^+) beams of 0.29, 0.42 and 0.54 A MeV through the ^3He gas target. These energies were selected so as to match with the velocities of the ^7Be recoils produced using 3.5, 5.2 and 6.6 MeV ^4He beams of our interest. The DRAGON separator was then tuned to select the Be nuclei in one of the possible charge states. The Faraday cups before the target chamber and after the first magnetic dipole of the separator [25] (having typical dark currents of 4 and 12 pA, respectively) were used for counting the Be nuclei and deducing the q_f values and the CSD. Our observations showed that for the

aforementioned energies, ~ 40 to 60% of the recoils had the 3^+ charge state at the exit of the gas target. The ${}^7\text{Be}$ recoils, with their velocities matched to that of ${}^9\text{Be}$, are expected to give the same results. For the gas target pressures of 1 and 5 Torr, the CSD of the Be nuclei were measured to be the same within the experimental uncertainties. Therefore, we conclude that an equilibrium in the CSD of Be nuclei was already reached below 1 Torr. Currently, we are estimating the errors in the values of q_f utilizing our measurements and the systematics from previous such measurements carried out at DRAGON [29]. In particular, the latter should help us deduce the lowest pressure at which the CSD reaches its equilibrium. It is worth noting that the ${}^4\text{He}$ (3^+) ion is not physically possible. Therefore, it is usually preferred to tune the DRAGON separator so as to select the ${}^7\text{Be}$ (3^+) recoils and achieve high suppression for the beam. The background contributions to $N_{7\text{Be}}^f$ were investigated in Ref. [24] using a ${}^4\text{He}$ beam of 6.6 MeV energy and a ${}^3\text{He}$ target. Figure 4 shows the DSSSD spectra from this work. The peak with an area of 11, 500 counts seen in Fig. 4(a) between 600 to 720 channels corresponds to ${}^7\text{Be}$ recoils. The total numbers of counts in the same region

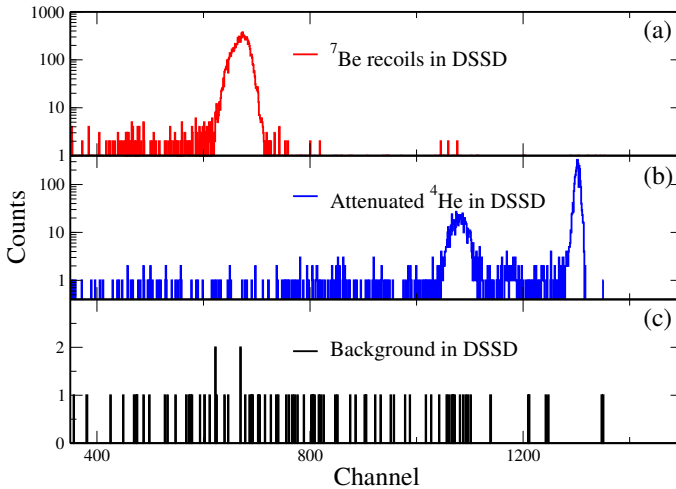


Fig. 4. Histograms of the particles detected simultaneously in any of the x and y -strips of the DSSSD during ~ 9 hour data collections [24]. (a) The spectrum corresponds to the measurement with a ${}^4\text{He}$ beam impinging on the ${}^3\text{He}$ target. The DRAGON separator was tuned to select the ${}^7\text{Be}$ (3^+) recoils. The spectra corresponding to the attenuated ${}^4\text{He}$ beam that was tuned to go through the separator and the background with no beam are shown in (b) and (c), respectively. Only negligible contributions from background with or without beam can be seen, for example, in between the channels 600 to 720, where the ${}^7\text{Be}$ recoil peak is present.

are relatively negligible both for the attenuated ${}^4\text{He}$ beam (Fig. 4(b)) and the background with no beam (Fig. 4(c)). Therefore, the background contributions to $N_{7\text{Be}}^f$ from these two sources can be ignored in this case. However, the two-dimensional ${}^7\text{Be}$ spectrum of energy *versus* identification number of the DSSSD strip from our more recent measurement indicates that the background could be different under different experimental conditions. See Fig. 5 for more details.

As discussed above, we are still at a preliminary stage of analysis and more refinements may be expected in the near future. After noting the levels of uncertainties in our results presented here, we would like to stress that the cross section measurements with accuracies better than 10% are feasible using our DRAGON setup.

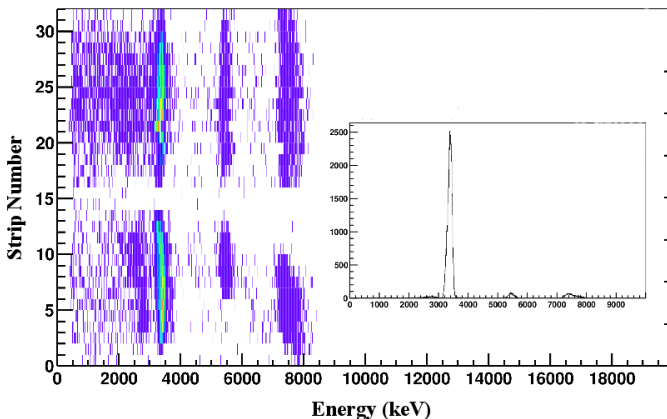


Fig. 5. The two-dimensional histogram of energy *versus* identification number for the vertical (0–15) and the horizontal (16–31) strips of the DSSSD. (Inset) The one-dimensional projection onto the x -axis. Therefore, it shows the combined energy spectrum for all of the strips. Three significant peaks can be seen apart from the intense ${}^7\text{Be}$ recoil peak around 3.4 MeV. The origin of these additional peaks and their influence on the error in $N_{7\text{Be}}^f$ are being investigated.

3. Discussion and future

From the summary presented in Fig. 1 and the description of our results in the preceding sections, it can be noted that further data are yet required in a wide energy range of $E_{\text{cm}} = 0.1$ to 3 MeV. In this regard, one should note that each of the aforementioned experimental techniques is suitable only to a limited energy range, therefore, the use of different methods becomes inevitable to obtain consistent data. In such situations, an overlap

in the energy range of different data sets is essential for a comparison of the results and consistent data evaluations. Furthermore, the data would be more reliable if different techniques could be simultaneously employed as in the case of the ERNA Collaboration. Clearly, future data motivated by these facts will play highly important roles. We would like to note that the three activity data points (Madrid'11) presented in Fig. 1 (d) are evenly distributed in the range of $E_{\text{cm}} = 1$ and 3 MeV and agree with the ERNA work. Supported by this result, our future work is planned at energies above 1 MeV so as to fix the energy dependence of the S_{34} -factor accurately [11].

Several observations can be made via a comparison between different calculations and the data sets, which could also help plan the future works to improve the accuracy in the value of $S_{34}(0)$. For example, some of the theoretical calculations have an overall apparent agreement with the available data for either the present reaction [19] or the ${}^3\text{H}(\alpha, \gamma){}^7\text{Li}$ ‘sister reaction’ [16] that has not been studied in recent years; but, none of the calculations are in simultaneous agreement with the data for both of these two reactions. Therefore, new measurements of the ‘sister reaction’ are strongly recommended for an evaluation of the theories. We also note that the discrepancies between any two different theoretical calculations for the cross sections of the two reactions become smaller when a common artificial scaling factor is used. Further theoretical work will be required in order to understand the origin of this scaling factor and compare different types of calculations [30]. In some cases, the theories can be modified to obtain a reasonable agreement between the calculations and the S_{34} data [14]. However, the ${}^3\text{He}(\alpha, \alpha){}^3\text{He}$ elastic scattering data obtained a few decades ago cannot be simultaneously reproduced by these calculations. Therefore, new measurements on this reaction are also strongly suggested. It is also worth stressing that some of the theoretical calculations have apparent differences in the s - and d -wave contributions to the S_{34} -factor [11]. To constrain theories and restrict the spread in the extrapolations, data of these contributions should be obtained by measuring the angular distribution of the prompt γ rays from the currently studied reaction.

In summary, focused efforts are yet required on the present reaction as well as the related reactions in order to quote a long sought after final value of $S_{34}(0)$ with the best possible accuracy.

We would like to thank T. Neff and K. Nollett for useful discussions on the status of the calculations. This work has been supported by the UK STFC and was partly financed by the Spanish Research Funding Agency CICYT under project FPA2009-07387 and CSIC-JAEdpredoc grant.

REFERENCES

- [1] H.D. Holmgren, R.L. Johnston, *Phys. Rev.* **113**, 1556 (1959).
- [2] E.G. Adelberger *et al.*, *Rev. Mod. Phys.* **83**, 195 (2011).
- [3] J. J ose, C. Iliadis, *Rep. Prog. Phys.* **74**, 096901 (2011).
- [4] P.D. Parker, R.W. Kavanagh, *Phys. Rev.* **131**, 2578 (1963).
- [5] H. Krawinkel *et al.*, *Z. Phys.* **A304**, 307 (1982).
- [6] E.G. Adelberger *et al.*, *Rev. Mod. Phys.* **70**, 1265 (1998).
- [7] B.S. Nara Singh *et al.*, *Phys. Rev. Lett.* **93**, 262503 (2004).
- [8] D. Bemmerer *et al.*, *Phys. Rev. Lett.* **97**, 122502 (2006).
- [9] F. Confortola *et al.*, *Phys. Rev.* **C75**, 065803 (2007).
- [10] T.A.D. Brown *et al.*, *Phys. Rev.* **C76**, 055801 (2007).
- [11] R.H. Cyburt, B. Davids, *Phys. Rev.* **C78**, 064614 (2008).
- [12] A. Di Leva *et al.*, *Phys. Rev. Lett.* **102**, 232502 (2009).
- [13] A. Di Leva *et al.*, *Nucl. Instrum. Methods Phys. Res.* **A595**, 381 (2008).
- [14] P. Mohr, *Phys. Rev.* **C79**, 065804 (2009).
- [15] T. Kajino, A. Arima, *Phys. Rev. Lett.* **52**, 739 (1984).
- [16] K.M. Nollett, *Phys. Rev.* **C63**, 054002 (2001).
- [17] P. Descouvemont *et al.*, *At. Data Nucl. Data Tables* **88**, 203 (2004).
- [18] R.H. Cyburt *et al.*, *J. Cosmol. Astropart. Phys.* **11**, 012 (2008).
- [19] T. Neff, *Phys. Rev. Lett.* **106**, 042502 (2011) and references therein.
- [20] A. Coc, *The Astrophys. J.* **744**, 158 (2012) and references therein.
- [21] C. Angulo *et al.*, *Nucl. Phys.* **A656**, 3 (1999).
- [22] M. Carmona-Gallardo *et al.*, *Phys. Rev.* **C86**, 032801(R) (2012) and references therein.
- [23] B.S. Nara Singh *et al.*, *J. Phys. Conf. Ser.* **337**, 012057 (2012).
- [24] S.K.L. Sjue *et al.*, *Nucl. Instrum. Methods Phys. Res.* **A700**, 179 (2013).
- [25] D.A. Hutcheon *et al.*, *Nucl. Instrum. Methods Phys. Res.* **A498**, 190 (2003).
- [26] Y. Nir-El *et al.*, *Phys. Rev.* **C75**, 012801 (2007).
- [27] D.R. Tilley *et al.*, *Nucl. Phys.* **A708**, 3 (2002),
<http://www.tunl.duke.edu/nuclldata/>
- [28] S. Reeve, M.Sc. Thesis, *Determining the Transmission Efficiency for ${}^3\text{He}(\alpha, \gamma){}^7\text{Be}$ in DRAGON*, August 2012.
- [29] W. Liu *et al.*, *Nucl. Instrum. Methods Phys. Res.* **A496**, 198 (2003).
- [30] K.M. Nollett, T. Neff, private communication.